

Differentiation of normal and cancerous lung tissues by multiphoton imaging

Chun-Chin Wang*

National Taiwan University
Institute of Biomedical Engineering
No. 1 Section 1 Jen-Ai Road
Taipei 100
Taiwan

Feng-Chieh Li*

Ruei-Jhih Wu

Vladimir A. Hovhannisyan

National Taiwan University
Department of Physics
No. 1 Section 1 Roosevelt Road
Taipei 10617
Taiwan

Wei-Chou Lin

National Taiwan University Hospital
Department of Pathology
No. 7 Chung-Shan S Road
Taipei 10617
Taiwan

Sung-Jan Lin

National Taiwan University
Institute of Biomedical Engineering
No. 1 Section 1 Jen-Ai Road
Taipei 100
Taiwan
and
National Taiwan University Hospital
Department of Dermatology
Taipei 100
Taiwan

Peter T. C. So

Massachusetts Institute of Technology
Department of Mechanical Engineering
500 Technology Square
Cambridge, Massachusetts 02139

Chen-Yuan Dong

National Taiwan University
Department of Physics
No. 1 Section 1 Roosevelt Road
Taipei 10617
Taiwan

1 Introduction

Lung carcinoma is the most prevalent form of cancer worldwide.¹ In Taiwan, the incidence of lung adenocarcinoma in Taiwan is 42.1% and 73.5% among all male and female lung cancer patients, respectively.² Clearly, the development

Abstract. We utilize multiphoton microscopy for the label-free diagnosis of noncancerous, lung adenocarcinoma (LAC), and lung squamous cell carcinoma (SCC) tissues from humans. Our results show that the combination of second-harmonic generation (SHG) and multiphoton excited autofluorescence (MAF) signals may be used to acquire morphological and quantitative information in discriminating cancerous from noncancerous lung tissues. Specifically, noncancerous lung tissues are largely fibrotic in structure, while cancerous specimens are composed primarily of tumor masses. Quantitative ratiometric analysis using MAF to SHG index (MAFSI) shows that the average MAFSI for noncancerous and LAC lung tissue pairs are 0.55 ± 0.23 and 0.87 ± 0.15 , respectively. In comparison, the MAFSIs for the noncancerous and SCC tissue pairs are 0.50 ± 0.12 and 0.72 ± 0.13 , respectively. Our study shows that nonlinear optical microscopy can assist in differentiating and diagnosing pulmonary cancer from noncancerous tissues. © 2009 Society of Photo-Optical Instrumentation Engineers. [DOI: 10.1117/1.3210768]

Keywords: multiphoton microscopy; autofluorescence; second-harmonic generation (SHG); lung adenocarcinoma (LAC); squamous cell carcinoma (SCC).

Paper 09100RR received Mar. 23, 2009; revised manuscript received Jun. 20, 2009; accepted for publication Jun. 23, 2009; published online Aug. 25, 2009.

*Authors contributed equally to this work.

Address all correspondence to: P. T. C. So, Department of Mechanical Engineering, Massachusetts Institute of Technology, Cambridge, MA 02139; Tel: 617-253-6552; Fax: 617-258-9346; E-mail: ptso@mit.edu; or Chen-Yuan Dong, Department of Physics, National Taiwan University, Taipei 10617, Taiwan; Tel: 886-2-3366-5155; Fax: 886-2-2363-9984; E-mail: cydong@phys.ntu.edu.tw

of a minimally invasive imaging modality for rapid, *ex vivo* or *in vivo* biopsy of this disease is of great medical significance. However, prior to performing *in vivo* endoscopic investigation for clinical application,³ it is necessary to image and characterize optical features of the chosen imaging technique for lung cancers under *ex vivo* conditions.

Due to the advantages of two-photon microscopy⁴ and other related nonlinear optical phenomena such as second-harmonic generation (SHG), researchers have demonstrated the potential applications of this methodology in disease di-

agnosis and characterization. For instance, three-dimensional (3-D) images of endogenous tissue fluorescence can be effectively used for distinguishing normal, precancerous, and cancerous epithelial tissues,⁵ detection of basal cell carcinoma (BCC),^{6,7} and determination of the structures of healthy and tumor collagen.⁸ Moreover, in intravital studies, 3-D high-resolution imaging of structural features and physiological function in tumors have been demonstrated.⁹ In addition, SHG signal generated from tumor may be used to estimate drug delivery characteristics.¹⁰ Furthermore, the movement of cancer cells along the extracellular matrix networks was also visualized.¹¹ The application of nonlinear optical microscopy is not limited to cancer-related studies. Other areas such as developmental biology, neurobiology, and orthopedics have also benefited from the advantages of nonlinear optical imaging.^{12–16}

In this work, we proposed to utilize nonlinear optical microscopy to image and analyze *ex vivo* noncancerous and cancerous lung tissues. Structurally, normal lung tissue is composed of collagen and elastic fibers, with the epithelium of the alveolus as cells responsible for gas exchange. On the other hand, cancers such as lung adenocarcinoma (LAC) and squamous cell carcinoma (SCC) are composed primarily of tumor masses. Since previous studies have shown that collagen fibers are effective in producing second-harmonic generation signal and elastic fibers along with cells [NAD(P)H, FAD] can be autofluorescent,¹³ multiphoton imaging may be effective in discriminating noncancerous and cancerous lung tissues.

2 Materials and Methods

Human lung specimens used in this investigation were obtained from the Tissue Bank Core Facility for Genomic Medicine of National Taiwan University Hospital. Those frozen tissues were stored in liquid nitrogen and include six matching pairs of noncancerous (NC)/LAC specimens and five matching pairs of NC/SCC tissues from the same patient. Each tissue block (approximately $3 \times 3 \times 1 \text{ mm}^3$ in volume) was placed on the slide, mounted carefully and covered with a coverslip (thickness 0.17 mm), and kept at room temperature for 10 min prior to imaging. The multiphoton imaging system utilized in this study is similar to one described previously.⁶ A commercial, tunable, Ti-sapphire pulsed laser (Tsunami; Spectra Physics, Mountain View, California) with a central wavelength of 760 or 780 nm was used as the excitation light source. The laser beam is scanned in the focal plane by a galvanometer-driven, *x-y* mirror scanning system (Model 6220, Cambridge Technology, Cambridge, Massachusetts). Upon entering the imaging upright microscope (E800, Nikon, Japan), the laser beam was beam-expanded and reflected into a high numerical aperture (NA), oil-immersion objective (S Fluor 40 \times , NA 1.3, Nikon) by a primary, short-pass dichroic mirror (700DCSPRUV, Chroma Technology, Rockingham, Vermont).

The average laser power irradiating the specimens was around 10 mW, and the multiphoton autofluorescence (MAF) and SHG signals produced at the focal volume are collected by the same focusing objective. Prior to reaching the single-photon counting photomultiplier tubes (R7400P, Hamamatsu, Hamamatsu City, Japan) and homebuilt discriminators, MAF

and SHG signals are separated into separate simultaneous detection channels. For LAC imaging, a secondary dichroic mirror (435DCXR, Chroma Technology) and two additional bandpass filters (HQ380/40 and 435LP/700SP) are used for the detection of SHG and broadband autofluorescence. The detection bandwidths for SHG and autofluorescence were 360 to 400 nm and 435 to 700 nm, respectively. For imaging tissues from the SCC patients, different dichroics (435DCXR, 495DCXR) and filter (HQ390/20, HQ465/70, HQ525/50) combinations were used to achieve the detection bandwidth of $390 \pm 10 \text{ nm}$ (SHG) and two MAF channels with bandwidths of 465 ± 35 and $525 \pm 25 \text{ nm}$. To acquire large area images of human lung tissues for comprehensive diagnosis, we used a sample positioning stage (Prior Scientific, Cambridge, UK) for specimen translation after each optical scan ($110 \times 110 \mu\text{m}^2$). In this manner, large area multiphoton images composed of 12 by 12 (total area: $1320 \times 1320 \mu\text{m}^2$ for LAC) and 10 by 10 (total area: $1100 \times 1100 \mu\text{m}^2$ for SCC) small-area optical images were achieved for each specimen. Public domain software ImageJ (National Institutes of Health, Bethesda, Maryland) was used to process raw images and signals. In addition, for data calculation of MAF to SHG index (MAFSI) results, the commercial software IDL (ITT Corporation, Washington, DC) was utilized. Furthermore, to correct for imaging field inhomogeneity, we used a home-written software, as described previously.¹⁷

In addition to qualitative imaging, we also used the quantitative metric of MAF to SHG index (MAFSI) for image analysis. This approach has been demonstrated to be useful in the quantitative analysis of basal cell carcinoma and differently aged skin.^{6,13} In short, MAFSI was determined by counting the number of pixels with MAF or SHG intensities above the chosen threshold levels. This approach was used to eliminate effects on detected signal levels due to scattering and specimen-induced spherical aberration. The pixel numbers of the MAF signal (MAF_p) and SHG signal (SHG_p) were then computed according to the ratiometric definition of $(MAF_p - SHG_p)/(MAF_p + SHG_p)$. According to this definition, MAFSI approaches the maximum value of 1 when only MAF signals are present, and MAFSI approaches -1 when only SHG signal is present. The MAFSI analysis on the LAC tissues was performed using broadband MAF, while that of the SCC tissues was achieved using the detection band of $465 \pm 35 \text{ nm}$.

3 Results and Discussion

Large-area and high-resolution multiphoton imaging was performed and representative images for noncancerous and LAC tissues are respectively shown in Figs. 1(a) and 1(b) (MAF: green) and SHG: blue). Morphologically, normal and cancerous lung tissues can be easily discriminated. First, the fibrillar architecture of collagen (solid white arrow) and elastic fibers (dashed white arrow) is found to be widespread within noncancerous lung tissue. The alveolus (enclosed region) and autofluorescent alveolar cells within (yellow arrow) representing the conformation of normal lung tissue can be easily delineated without extrinsic labeling. In comparison, the cancerous specimens are primarily composed of cellular masses. For comparison, histological images from the noncancerous and LAC tissues are respectively shown in Figs. 1(c) and 1(d).

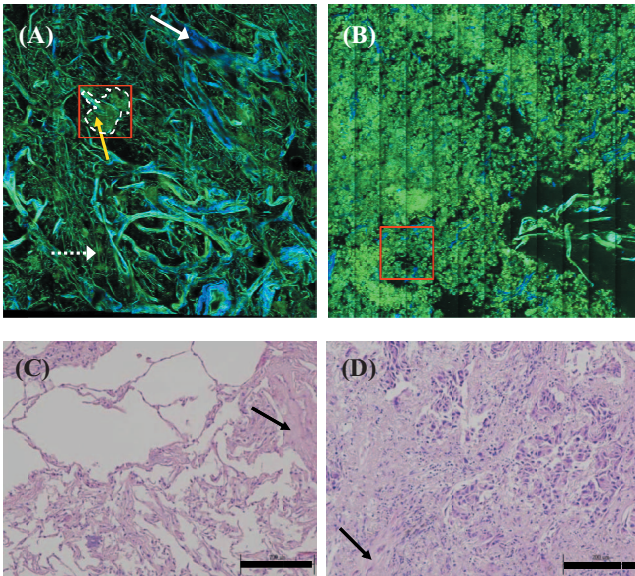


Fig. 1 Large area imaging ($1320 \times 1320 \mu\text{m}^2$) of (a) noncancerous lung and (b) LAC specimens. H&E stain of (c) noncancerous lung and (d) LAC specimens. Scale bar is $200 \mu\text{m}$.

Furthermore, more SHG signal is observed in noncancerous than in LAC tissues. To better discriminate noncancerous and cancerous lung specimens, selected regions of interest (boxed areas) in Figs. 1(a) and 1(b) are magnified and are respectively shown in Figs. 2(a) and 2(b). Several prominent features stand out. Note that in noncancerous lung tissue [Fig. 2(a)], the collagen and elastic fibers surrounding an alveolus are well defined. Furthermore, alveolar cells can be identified by MAF imaging and are fairly uniform in size and appearance. In contrast, multiphoton imaging of the LAC specimen in Fig. 2(b) shows that the fibrotic connective tissues found in noncancerous tissues are missing and that the imaged cells are irregular in shapes and sizes. In addition, cells undergoing mitosis (red arrow) can be identified, indicating the rapid growth of the cancer. Therefore, label-free, qualitative multiphoton imaging is effective in identifying features of LAC tissues whose normal counterparts are composed largely of fibrotic connective tissues.

In addition to comparing morphological differences, the MAFSI value can also yield quantitative comparison for cancer diagnosis. Assuming that the index distribution can be

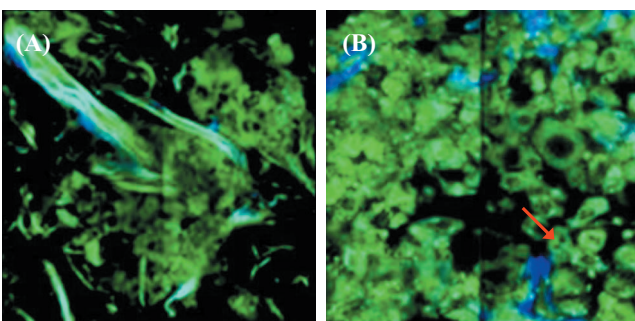


Fig. 2 (a) and (b) are magnified images from selected regions of interest in Figs. 1(a) and 1(b) respectively. Image size: $220 \times 220 \mu\text{m}^2$.

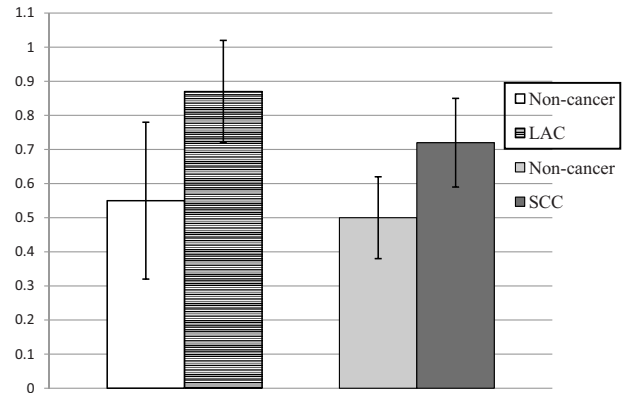


Fig. 3 Average MAFSI value along with standard deviation for non-cancerous lung, LAC, and SCC tissues.

approximated to be Gaussian, the average and standard deviation of MAFSI from the six matching pairs of NC/LAC and five matching pairs of the NC/SCC tissues can be calculated. Figure 3 along with Table 1 show that the average MAFSI for NC and LAC tissues are 0.55 ± 0.23 and 0.87 ± 0.15 , respectively. In comparison, the MAFSIs for the NC/SCC tissues are respectively 0.50 ± 0.12 and 0.72 ± 0.13 . The lower MAFSI value found for noncancerous tissues indicates the fact that noncancerous tissues contain a higher content of second-harmonic generating collagen fibers, an observation consistent with the morphological images of Figs. 1 and 2. However, both Fig. 3 and Table 1 show that the errors of the MAFSI indices are sufficiently large. This may be due, in part, to the fact that imaging was performed on collapsed lung tissues. Therefore, in future clinical applications, both the MAFSI index and multiphoton images need to be used for diagnostic purposes.

4 Conclusion

We have demonstrated that multiphoton autofluorescence and second-harmonic generation imaging may be effective in differentiating noncancerous from lung adenocarcinoma (LAC) and squamous cell carcinoma (SCC) tissues under label-free, *ex vivo* conditions. Noncancerous lung tissues contain collagen and elastic fibers with alveolar epithelial cells that are uniform in appearance and size. On the contrary, lung adenocarcinoma tissues lack fibrotic connective tissues and are composed of tumor masses. In addition, cells undergoing mitosis can be observed. Quantitative analysis using the multiphoton autofluorescence to second-harmonic generation index (MAFSI) supports the morphological images by measuring a lower overall second-harmonic generation signal within LAC and SCC tissues. Our work demonstrates the feasibility of using multiphoton imaging in rapid, *ex vivo* cancer biopsy in tissues whose normal structures are rich in connective fibers and suggests the possibility of applying multiphoton microscopy for rapid *ex vivo* tissue diagnosis or implementing multiphoton endoscopes for *in vivo* cancer diagnosis and surgery guiding in the future.

Table 1 MAFSI values for noncancerous, LAC, and SCC human lung tissues for the six- and five-pair specimens imaged. Averaged MAFSI values are also shown.

Tissue type	Specimen no.						Average
	1	2	3	4	5	6	
Noncancerous	0.26±0.17	0.75±0.11	0.81±0.16	0.42±0.16	0.72±0.16	0.35±0.16	0.55±0.23
LAC	0.57±0.26 (grade 1)	0.87±0.13 (grade 2)	0.93±0.17 (grade 2)	0.99±0.01 (grade 3)	0.95±0.03 (grade 3)	0.95±0.06 (grade 3)	0.87±0.15
Noncancerous	0.31±0.12	0.57±0.13	0.45±0.15	0.62±0.17	0.53±0.09		0.50±0.12
SCC	0.62±0.16 (grade 1)	0.61±0.13 (grade 1)	0.69±0.18 (grade 2)	0.77±0.12 (grade 3)	0.91±0.06 (grade 3)		0.72±0.13

Acknowledgments

This work was supported by the National Research Program for Genomic Medicine (NRPGM) of the National Science Council (NSC) in Taiwan and was completed in the Optical Molecular Imaging Microscopy Core Facility (A5) of NRPGM. We would also like to acknowledge the Tissue Bank Core Facility for Genomic Medicine of NTUH for providing the human lung tissue specimens.

References

- D. M. Parkin, F. Bray, J. Ferlay, and P. Pisani, "Global cancer statistics, 2002," *CA Cancer J. Clin.* **55**, 74–108 (2005).
- K. Y. Chen, C. H. Chang, C. J. Yu, S. H. Kuo, and P. C. Yang, "Distribution according to histologic type and outcome by gender and age group in Taiwanese patients with lung carcinoma," *Cancer* **103**, 2566–2574 (2005).
- L. Fu, A. Jain, C. Cranfield, H. K. Xie, and M. Gu, "Three-dimensional nonlinear optical endoscopy," *J. Biomed. Opt.* **12**(4), 040501-1–3 (2007).
- W. Denk, J. H. Strickler, and W. W. Webb, "2-photon laser scanning fluorescence microscopy," *Science* **248**, 73–76 (1990).
- M. C. Skala, J. M. Squirrell, K. M. Vrotsos, V. C. Eickhoff, A. Gendron-Fitzpatrick, K. W. Eliceiri, and N. Ramanujam, "Multiphoton microscopy of endogenous fluorescence differentiates normal, precancerous, and cancerous squamous epithelial tissues," *Cancer Res.* **65**, 1180–1186 (2005).
- S. J. Lin, S. H. Jee, C. J. Kuo, R. J. Wu, W. C. Lin, J. S. Chen, Y. H. Liao, C. J. Hsu, T. F. Tsai, Y. F. Chen, and C. Y. Dong, "Discrimination of basal cell carcinoma from normal dermal stroma by quantitative multiphoton imaging," *Opt. Lett.* **31**, 2756–2758 (2006).
- R. Cicchi, D. Massi, S. Sestini, P. Carli, V. De Giorgi, T. Lotti, and F. S. Pavone, "Multidimensional non-linear laser imaging of basal cell carcinoma," *Opt. Express* **15**, 10135–10148 (2007).
- X. Han, R. M. Burke, M. L. Zettel, P. Tang, and E. B. Brown, "Second harmonic properties of tumor collagen: determining the structural relationship between reactive stroma and healthy stroma," *Opt. Express* **16**, 1846–1859 (2008).
- E. B. Brown, R. B. Campbell, Y. Tsuzuki, L. Xu, P. Carmeliet, D. Fukumura, and R. K. Jain, "In vivo measurement of gene expression, angiogenesis, and physiological function in tumors using multiphoton laser scanning microscopy," *Nat. Med.* **7**(7), 864–868 (2001).
- E. Brown, T. McKee, E. diTomaso, A. Pluen, B. Seed, Y. Boucher, and R. K. Jain, "Dynamic imaging of collagen and its modulation in tumors in vivo using second-harmonic generation," *Nat. Med.* **9**, 796–800 (2003).
- J. Condeelis and J. E. Segall, "Intravital imaging of cell movement in tumours," *Nat. Rev. Cancer* **3**, 921–930 (2003).
- W. Supatto, D. Debarre, B. Moulia, E. Brouzes, J. L. Martin, E. Farge, and E. Beaurepaire, "In vivo modulation of morphogenetic movements in Drosophila embryos with femtosecond laser pulses," *Proc. Natl. Acad. Sci. U.S.A.* **102**, 1047–1052 (2005).
- S. J. Lin, R. J. Wu, H. Y. Tan, W. Lo, W. C. Lin, T. H. Young, C. J. Hsu, J. S. Chen, S. H. Jee, and C. Y. Dong, "Evaluating cutaneous photoaging by use of multiphoton fluorescence and second-harmonic generation microscopy," *Opt. Lett.* **30**, 2275–2277 (2005).
- K. A. Kasichke, H. D. Vishwasrao, P. J. Fisher, W. R. Zipfel, and W. W. Webb, "Neural activity triggers neuronal oxidative metabolism followed by astrocytic glycolysis," *Science* **305**, 99–103 (2004).
- K. Konig and I. Riemann, "High-resolution multiphoton tomography of human skin with subcellular spatial resolution and picosecond time resolution," *J. Biomed. Opt.* **8**, 432–439 (2003).
- R. LaComb, O. Nadiarykh, and P. J. Campagnola, "Quantitative second harmonic generation imaging of the diseased state osteogenesis imperfecta: experiment and simulation," *Biophys. J.* **94**, 4504–4514 (2008).
- V. A. Hovhannisyan, P. J. Su, Y. F. Chen, and C. Y. Dong, "Image heterogeneity correction in large-area, three-dimensional multiphoton microscopy," *Opt. Express* **16**, 5107–5117 (2008).